Journal of Signal Processing Systems (2018) 90:1205–1211
https://doi.org/10.1007/s11265-017-1308-9

An Effective Segmentation Method for MRI Images Based on TV-L1 and GVF Model

Yuefeng Zhao[1] · Xiaofei Li[1] · Weili Wang[1] · Xiaoxiao Pan[1] · Chaoying Yuan[1] · Xiaomei Guan[1] · Dongmei Wei[1]

Received: 21 July 2017 / Revised: 25 October 2017 / Accepted: 13 November 2017 / Published online: 2 December 2017

Abstract
Liver magnetic resonance imaging (MRI) is of vital importance for computer-aided diagnosis and it is equally important in liver surgery planning. In this paper, accurate contours of the liver in MRI images automatically for subsequent adaptive radiation therapy can be extracted by the work. It is consisted of three components. Firstly, noise and artifacts are removed from the MRI image by an edge-preserving filtering using total variation with L1 norm (TV-L1). Secondly, the wavelet parameters are calculated at different levels of scale, and then the initial contour of the liver is obtained at the appropriate scale. And finally the precise liver structure is extracted by the gradient vector flow (GVF) model converging to the initial contour. The accuracy of the segmentation results are verified by comparing with the manually ones. For clinical cases, the numerical results illustrates enough accuracy and robustness for medical environments. And it also has a reasonable computational cost.

Keywords Total variation with L1 · Wavelet edge detection · Gradient vector flow · Magnetic resonance imaging

1 Introduction

Recently, the study of liver images has been widely used in clinical practice, and has become one of the important means for doctors to carry out liver physiological function, medical inspection items, pathological and anatomical research. Liver border verification is a prerequisite for quantitative analysis and diagnosis, and has important research value. At present, Computed Tomography (CT) applied for liver segmentation has been widely proposed. On the contrary, MRI image has not been widely used for it, while the MRI image is powerful imaging tool in helping liver segmentation. The segmentation of a region of interest (ROI) in MRI images, such as a sensitive structure or a tumor target volume, is an important task in radiotherapy [1–3]. Compared to Computed Tomography (CT), there is no X radiation for MRI. Imaging modalities like Computed Tomography (CT) do not allow a noninvasive direct visualization of the individual liver segments. Segment boundaries can only be approximated by the corresponding liver vessels [4]. Importantly, MRI has multi-sequence capabilities (e.g., diffusion weighted imaging and perfusion weighted imaging).

In recent years, the need for efficient and robust segmentation tools is increasing. Techniques include the use of deformable model, sparse shape model [5], and image registration [6]. However, the two limitations hinder the segmentation. MRI is still subject to random noise, partial volume effect and gray level bias field in the imaging process [7]. The accuracy of the segmented contours may be compromised. In addition, with the numbers of images increasing, it becomes impractical to manually segment the ROIs slice by slice. This requires the development of new automated segmentation techniques or schemes for MRI date segmentation.

To perform quantitative analysis using MRI images, segmentation of structures such as the liver and tumor is required. Traditional segmentation of MRI date is extremely tedious, time consuming, and suffers user variability. In this paper, we propose a novel method that

✉ Yuefeng Zhao
yuefengzhao@126.com

✉ Chaoying Yuan
1157957227@qq.com

✉ Xiaomei Guan
qianjiangyanran@163.com

✉ Dongmei Wei
weidongmei@163.com

[1] School of Physics and Electronics, Shandong Normal University, Jinan, China

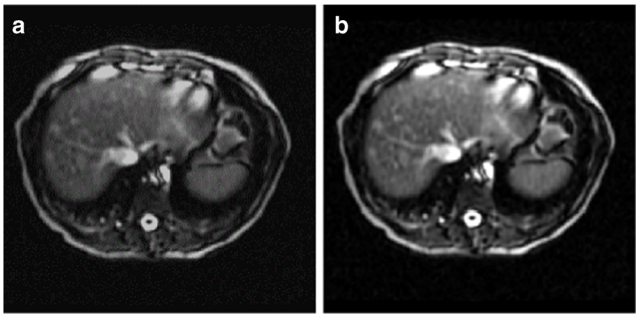

Figure 1 Image smoothing denoising processing. **a** The original MRI image of liver; **b** The MRI image of liver after pre-processing.

the artifacts and noise are removed from the MRI image by an edge-preserving filtering using TV-L1 model [8, 9]. Secondly calculate the wavelet parameters at different levels of scale, and then find appropriate parameter for testing to get initial liver region. At the last stage, the liver structure is convergent by GVF model [10, 11]. The experimental results demonstrate a very promising performance of the method which requires less of the clinician's time, and has enough accuracy and robustness for medical environments.

The liver segmentation based GVF applied to the MRI images can be described as follows. Firstly, the doctors manually segment patient slice data to find out the liver contour and construct the narrow band, as the template image. Secondly, the operators extract another slice of the same patient and preprocess the image to remove the noise and eliminate the artifacts. Thirdly, the template image contour is mapped to the target image by multi-scale B spline registration to find the initial contour. Finally, the narrow band is constructed again, and the edge curve is further refined by GVF model, then the precise contours can be got.

The main contribution of this paper can be summarized as follows: (I) Segmentation method to auto-propagate contours is proposed for MRI image. (II) A multi-scale wavelet edge detection based on GVF method is proposed. This framework can effectively avoid the difficulties in liver image segmentation and alleviate the affection of random noise, partial volume effect and gray level bias field in the imaging process. Finally, it can achieve better performance.

2 Methodology

2.1 Pre-Processing MRI Images by TV-L1 Model

The analysis and diagnosis of magnetic resonance imaging are complex,the local lesion performed differently in different models, it was black on MRI images, and on some other images it was white. The difference depends not only on the inherent characteristics of the tissue, but also on the imaging technology. Furthermore, the inherent characteristics of tissue vary with the magnetic field intensity of MRI scanner. Although MRI images have many advantages, MRI is still affected by random noise, local volume effect and gray bias field due to the limitation of imaging conditions and technical constraints, therefore, the edges and inflection points of objects in images are difficult to be accurately defined. For a specially appointed image, the original images are preprocessed in order to reduce the noise and enhance the image contrast and fusion degree, as shown in Fig. 1.

Image is an important source of information. Most of abdominal MRI images are noisy and the edges of objects are not clear enough. MRI image process is still subject to random noise, partial volume effects and the impact of gray bias field. Hence the usual segmentation algorithms, leads to not only recognizing main edges, but also extracting additional boundaries. To handle this problem, we applied pre-processing stage to the input image before applying the main segmentation stage. In this paper, the artifacts and noise are removed from the MRI image by TV-L1.

TV-L1 is a very powerful tool to enhance the boundaries and the image contrast in medical images. It is possible to significantly reduce noise and improve edge information, making them more suitable for edge detection. Darbon's analysis [12] of the discrete TV-L1 model is used as a contrast invariant filter. Using this algorithm we know that the TV-L1 model is able to separate image features according to their scales, where the scale is analytically defined by the multi-scale analysis. For a given target image, the first pre-processing can remove noise and enhance the image contrast and degree of integration as shown in Fig. 2.

The TV-L1 model (1) acts on the simple 2-dimensional image

$$\mathrm{f} = \mathrm{b1Br}(0) \tag{1}$$

which has intensity $\mathrm{b} > 0$ at all points (m_1, m_2) inside the disk $\mathrm{Br}(0) = \left\{(m_1, m_2) : m_1^2 + m_2^2 \leq r^2\right\}$ and intensity 0 everywhere else.

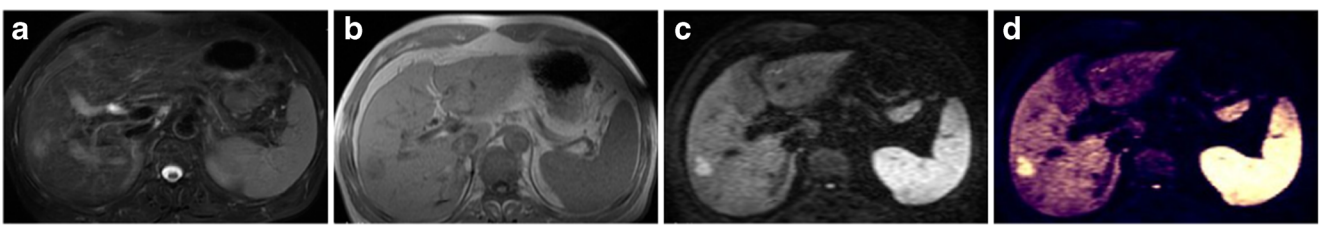

Figure 2 Image pre-processing. **a** Original image; **b** change gray values; **c** TV-L1 model process; **d** enhance contrast.

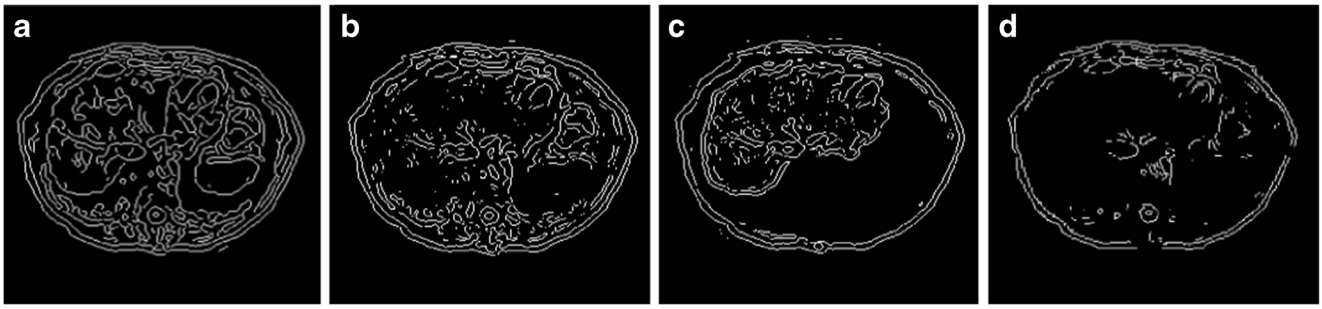

Figure 3 Liver shape extracted by different scale parameter λ. (λ = 0.8, 0.6, 0.4, 0.2 from (**a**) to (**d**)).

Chan and Esedoglu showed that for this *f*, solving (2) gives

$$u_\lambda^* \begin{cases} 0 & if\ 0 < \lambda < \frac{2}{r}, \\ b\ for\ any\ b \in [0,1] & if\ \lambda = \frac{2}{r}, \\ f & if\ \lambda > \frac{2}{r}, \end{cases} \tag{2}$$

In general the TV-L1 solution is unique. In the case of the above disk, if $\lambda = 2/r$, problem (2) has a very small infinite. Small-scale λ is corresponding to the high-frequency signal, and large-scale λ corresponding to the low-frequency signal. The TV-L1 energy of a function *f* can be expressed as an integral of the geometry energies of the superlevel sets of f, i.e.,(3)

$$\mathrm{E}(\mathrm{n}, \lambda, \mathrm{f}) = \int_{-\infty}^{\infty} E_G(L(n,\mu);\lambda, L(f,\mu))d\mu \tag{3}$$

Formula (3), known as the layer cake formula [13], can be combined with coarea formula $\int |\nabla_{\mathrm{n}}| = \int_{-\infty}^{\infty} Per(L(n,\mu))d_\mu$ with the formula $\int |\mathrm{n}-\mathrm{f}|\, d_x = \int_{-\infty}^{\infty} |\mathrm{L}(\mathrm{n},\mu)\Delta\mathrm{L}(\mathrm{f},\mu)|\, d_\mu$.

2.2 Multi-Scale Wavelet Edge Detection

Multi-scale analysis is a property of the wavelet transform and a signal on a range of different levels of decomposition analysis space [14]. Small-scale is corresponding to the high-frequency signal with high temporal resolution, and large-scale corresponding to the low-frequency signal with domain high resolution. Actually, the image is limited on some scales using wavelet decomposition, and Fig. 3 shows the wavelet edge extraction at different scales. The wavelet transform decomposes the image into two parts: the low frequency information and high frequency information. The low-frequency information of the frame image accounts for most of all the information, and the details of the high-frequency image information, such as the edge and the noise, a small portion of the total information. This is a one-dimensional decomposition of the image [15]. On the basis of the one-dimensional information, the high frequency part is decomposed further into two parts: low frequency and high frequency. In the two-dimensional case, a two-dimensional φ(x, y) and three-dimensional scaling wavelet functionφ^1(x, y), φ^2(x, y), φ^3(x, y) are employed. Each is a product of one-dimensional scaling functions and corresponding wavelet function, resulting in a separable scaling function φ(x, y) = φ(x)ϕ(y), i.e. the direction of the sensitive separable wavelet function:

$$\begin{aligned} \varphi^1(x,y) &= \varphi(x)\varphi(y) \\ \varphi^2(x,y) &= \varphi(x)\varphi(y) \\ \varphi^3(x,y) &= \varphi(x)\varphi(y) \end{aligned} \tag{4}$$

φ^1(x, y) represents a measure of the gray-scale variation in the horizontal direction, φ^2(x, y) represents a measure of the gray-scale variation in the vertical direction, φ^3(x, y) represents a measure of the gray-scale variation in the diagonal direction.

Multi-scale analysis is a property of the wavelet transform and a signal on a range of different levels of decomposition analysis space. Small-scale λ is corresponding to the high-frequency signal with high temporal resolution, and large-scale λ corresponding to the low-frequency signal with domain high resolution.

2.3 GVF Model Guidance Convergence

The initial contour is obtained by wavelet transform, but the edge is rough and the liver is extremely complex shapes. Due to some particularly deep depressions on MRI images, this paper selected edge convergence GVF model [16–18]. GVF

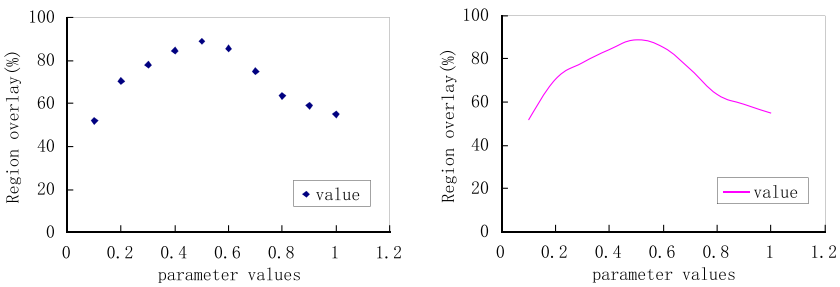

Figure 4 Coincidence rate of different scales of parameter λ. **a** Parameter λ of different scales of the coincidence rate distribution. **b** The curve fitting of scale parameter λ.

Table 1 Comparison of the segmentation accuracy between sparse shape model and our method.

method	sparse shape model	our method
Accuracy (%)	70.4012	72.6518

guide the convergence process is the process of finding the minimum point of the energy function, starting from the initial position of the artificial definition, deformed at decreasing energy function algorithm driven until it reaches the edge of the target. Define the value of the gradient vector field is obtained by minimizing the energy function to measureV(x, y) = (u(x, y), v(x, y)). Energy function equation is as follows:

$$\varepsilon = \mu\int\left(\mu_x^2 + \mu_y^2 + \nu_x^2 + \upsilon_y^2\right) + |\nabla f|^2 |V-\nabla f|^2 dxdy \quad (5)$$

From the view of numerical evaluation, there are some shortcomings in the GVF model. Firstly, the evolved curves or surfaces need to be embedded into another high dimensional layer, and it is very complicated and very cumbersome steps. Secondly, the GVF model will soon deviate from the signed distance function in the process of evolution and need to initialize the contour line frequently, however, the initialization is a very time-consuming process.

To remedy the defect, in this paper, we proposed a method to construct the GVF model under the guidance of narrowband construction, and the computation is controlled in the neighborhood of the contour curve, so that not only can reduce the amount of calculation, but also retain the advantages of GVF topology. A narrow bandwidth of 2D is constructed on the contour curve extracted based on the wavelet edge analysis.

The specific algorithm is described as follows:

(1) MRI image pre-processing, artificial segmentation, building narrow band;
(2) Finding the control points based on multi-scale features, and the initial contour of liver is found by B spline mapping, and then constructing the narrow band again;
(3) Setting the narrow point close to the boundary point as the observation point;

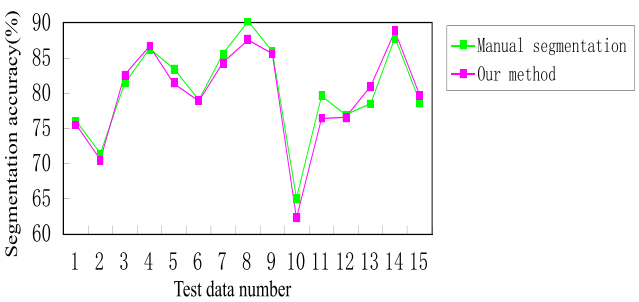

Figure 5 Comparison of test data segmentation accuracy.

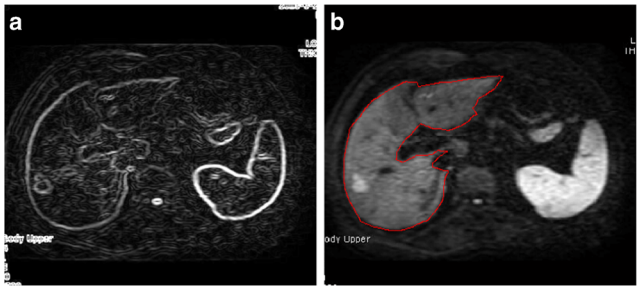

Figure 6 Edge detection chart. **a** The initial contour is extracted by wavelet edge detection based on TV-LI. **b** The liver structure is obtained by the GVF model convergence.

(4) Fixed a boundary point; and then obtained the curve equation of the non-boundary points in the narrow band at the next moment according to the GVF deformation model, until the curve evolves to the observation point;
(5) The GVF model eventually converges to all the boundary points in the narrow band.

3 Results and Discussion

3.1 Experimental Configuration

We introduce Dice Similarity Index (DSI) coefficient for further quantitative analysis [19–23]. DSI coefficient is a measure of automatic segmentation and manual segmentation in line with the degree of quantized coefficients, which is typically used to assess the similarity of the results of the computer division and medical experts with extensive experience in providing image segmentation data sets. DSI higher coefficient closer illustrated with hand-cut, split more accurate segmentation results if DSI coefficient greater than 70% is considered to manual segmentation results with better consistency. Its formula can be expressed as (6)

$$D(E, F) = 2 \times |E \cap F| / (|E| + |F|) \times 100\% \quad (6)$$

where E represents the medical experts hand-cut image, F represents the results of image segmentation algorithm, $|E \cap F|$ represents the two images overlap represents the number of pixels, $|E|$ and $|F|$ represent the number of pixels in each of the two images. As shown in Fig. 4, MRI images by calculating the automatic liver segmentation results DSI coefficient can reach 89.39% when $\lambda = 0.497$, it can be regarded as an effective segmentation.

3.2 Experimental Analysis

3.2.1 Contrast Analysis

The method proposed in this paper is simple in operation and can be used in automatic segmentation. Sparse matrix model,

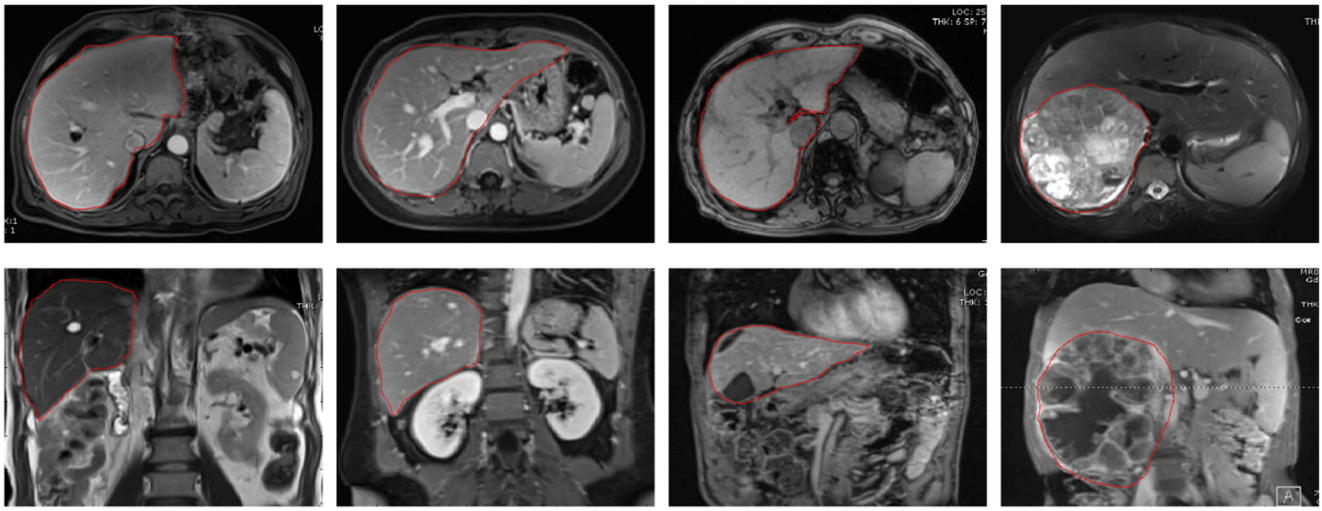

Figure 7 Original image and final mask in red from datasets. The first row is transverse view, the second row is coronal view.

often need to build the probability map, so that the edge is expressed as a sparse equation, not targeted and very long time. The comparison of the segmentation accuracy based on sparse method and the method of this paper is as Table 1.

Fifteen sets of test data were selected, and compared with the clinical data of the experts to verify the correction of the picture, to verify the effectiveness of the proposed method in this paper. Segmentation contrast accuracy as shown in Fig. 5.

3.2.2 Clinical Application

We can get the ROI through the three steps, as shown in Fig. 6, this method requires less of the clinician's time, has enough accuracy and robustness for medical environments, and has a reasonable computational cost. Firstly, the original image is pre-treated by TV model, and the contrast of image is enhanced, and an initial contour is obtained. Secondly, the optimal parameters of the scale are calculated, and the image is decomposed under the best parameters, so as to compensate for the missing details in the pre-processing. Eventually, the liver structures is convergent by GVF model.

The method proposed in this paper is applied to the clinical segmentation of the region of interest, as shown in Fig. 7.

4 Conclusion

In this work we have developed a segmentation method to auto-propagate contours for MRI image. This paper processes MRI images by TV-L1model and a multi-scale wavelet edge detection based on GVF method. The fast establishment of narrow band and the convergence of GVF model in narrow band are based on the minimization of the energy function value of the gradient vector field. Near the narrow band, the NBR-GVF model converges to the minimum state of energy more quickly and accurately, enhances the adaptability of the segmentation, and reduces the number of iterations of GVF. Compared with sparse shape model approaches, the proposed method shows enough accuracy and robustness for medical environments, and has a reasonable computational cost.

Acknowledgments The research work was supported by National Natural Science foundation of China (Grant: 81400285).And the authors would also like to gratefully acknowledge the support from the key research and development foundation of Shandong Province (Grant: 2016GGX101016).

Author Contributions The experiment is approved by School of Physics and Electronics, Shandong Normal University. Yuefeng Zhao made the experimental design. Xiaofei Li and Weili Wang carried out the experimental work, data collection. Xiaofei Li, Xiaoxiao Pan and Chaoying Yuan participated data analysis and the preparation of the manuscript. Dongmei Wei participated in the experimental design, analysis of data and theoretical analysis. And all the authors reviewed the final manuscript.

Compliance with Ethical Standards

Competing Financial Interests The authors declare no competing financial interests.

References

1. López mir, F., Naranjo, V., Angulo, J., et al. (2014). Liver segmentation in MRI: A fully automatic method based on stochastic partitions. Computer Methods & Programs in. *Biomedicine, 114*(1), 11–28.
2. Masoumi, H., Behrad, A., Pourmina, M. A., et al. (2012). Automatic liver segmentation in MRI images using an iterative watershed algorithm and artificial neural network. *Biomedical Signal Processing and Control, 7*(5), 429–437.
3. Bereciartua, A., Picon, A., Galdran, A., et al. (2015). Automatic 3D model-based method for liver segmentation in MRI based on active contours and total variation minimization. *Biomedical Signal Processing and Control, 20*, 71–77.
4. Beichel, R., Pock, T., Janko, C., et al. (2015). Liver segment approximation in CT data for surgical resection planning[J].

Proceedings of SPIE - the. *International Society for Optical Engineering, 5370*, 1435–1446.
5. Aghasi, A., & Romberg, J. (2013). Sparse shape reconstruction. *SIAM Journal on Imaging Sciences, 6*(4), 2075–2108.
6. Lu, H., Beisteiner, R., Nolte, L. P., et al. (2013). Hierarchical segmentation-assisted multimodal registration for MR brain images. Computerized Medical Imaging & Graphics the official journal of the computerized medical imaging. *Society, 37*(3), 234–244.
7. Pavliha, D., Mušič, M. M., Serša, G., et al. (2013). Electroporation-based treatment planning for deep-seated tumors based on automatic liver segmentation of MRI images. *PLoS One, 8*(8), 1–13.
8. Micchelli, C. A., Shen, L., Xu, Y., et al. (2013). Proximity algorithms for the L1/TV image denoising model. *Advances in Computational Mathematics, 38*(2), 401–426.
9. Mohr, H., Wolfensteller, U., Frimmel, S., et al. (2015). Sparse regularization techniques provide novel insights into outcome integration processes. *NeuroImage, 104*, 163–176.
10. Zhang, F., Zhang, X., Cao, K., et al. (2012). Contour extraction of gait recognition based on improved GVF snake model. *Computers and Electrical Engineering, 38*(4), 882–890.
11. Rana, P. K., Dash, M. K., Routray, A., et al. (2011). Prediction of sea ice edge in the Antarctic using GVF snake model. *Journal of the Geological Society of India, 78*(2), 99–108.
12. Yin, W., Goldfarb, D., & Osher, S. (2013). The total variation regularized L 1 model for multiscale decomposition, multiscale model. Siam journal on. *Multiscale Modeling and Simulation, 6*(1), 190–211.
13. Chan, T. F., & EsedogLu, S. (2005). Aspects of total variation regularized $Lsp 1$ function approximation. *SIAM Journal on Applied Mathematics, 65*(5), 1817–1837.
14. Swaminathan, A., & Ramapackiyam, S. S. K. (2014). Edge detection for illumination varying images using wavelet similarity. *IET Image Processing, 8*(5), 261–268.
15. Dinov, I. D., Boscardin, J. W., Mega, M. S., et al. (2005). A wavelet-based statistical analysis of FMRI data: I. Motivation and data distribution modeling. *Neuroinformatics, 3*(4), 319–342.
16. Zhang, L., Parrini, S., Freschi, C., et al. (2014). 3D ultrasound centerline tracking of abdominal vessels for endovascular navigation. *International Journal of Computer Assisted Radiology and Surgery, 9*(1), 127–135.
17. Hafiane, A., Vieyres, P., & Delbos, A. (2014). Phase-based probabilistic active contour for nerve detection in ultrasound images for regional anesthesia. Computers in biology. *Medicine, 52*(3), 88–95.
18. Liu, H. T., Sheu, T. W., & Chang, H. H. (2013). Automatic segmentation of brain MR images using an adaptive balloon snake model with fuzzy classification. *Medical & Biological Engineering & Computing, 51*(10), 1091–1104.
19. Aribi, Y., Hamza, F., Wali, A., et al. (2014). An automated system for the segmentation of dynamic Scintigraphic images. *Applied Medical Informatics, 34*(2), 1–12.
20. Wedeen, V. J., Wang, R. P., Schmahmann, J. D., et al. (2008). Diffusion spectrum magnetic resonance imaging (DSI) tractography of crossing fibers. *NeuroImage, 41*(4), 1267–1277.
21. Gai, K., Qiu, M., Ming, Z., et al. (2017). Spoofing-jamming attack strategy using optimal power distributions in wireless smart grid networks. *IEEE Transactions on Smart Grid, 99*, 1–1.
22. Gai, K., Qiu, L., Chen, M., et al. (2017). SA-EAST: Security-aware efficient data transmission for ITS in mobile heterogeneous cloud computing. *ACM Transactions on Embedded Computing Systems, 16*(2), 1–22.
23. Qiu, M., Gai, K., & Xiong, Z. (2017). Privacy-preserving wireless communications using bipartite matching in social big data. *Future Generation Computer Systems*, 1–10. https://doi.org/10.1016/j.future.2017.08.004.

Yuefeng Zhao received the Ph.D. degrees from the Anhui Institute of Optics and Fine Mechanics (AIOFM), Chinese Academy of Sciences (CAS). His current position is a vice professor teaching in the School of physics and electronics, Shandong Normal University. His current research interests are RAMAN gain lidar to detect the tropospheric carbon dioxide concentration(41105008) which is supported by National Natural Science Foundation of China, and the measurement of based on frequency modulation optical fiber with the support from the key research and development foundation of Shandong Province under Grant No. 2009GG10004033.

Xiaofei Li is a master student at School of physics and Electronics, Shandong Normal University. Her research interest now is machine learning and Brain MRI images processing.

Weili Wang is a master student at School of physics and Electronics, Shandong Normal University. His Special field of interest is Spectral imaging technology in Handwriting Detection.

Xiaoxiao Pan is a master student at School of physics and Electronics, Shandong Normal University. Her research interest now is Surface-enhanced Raman scattering molecule separation and detection. She has published papers in international journal.

Xiaomei Guan is a master student at School of physics and Electronics, Shandong Normal University, Jinan, China. Her research interest now is the application of hyperspectral imaging technology in agriculture and MRI images processing.

Chaoying Yuan has graduated from School of Physics and Electronics, Shandong Normal University and now is a doctoral student at Beijing University of Posts and Telecommunications. Her Special field of interest included MRI image segmentation and signal communication.

Dongmei Wei received the Ph.D. degrees from the Shandong University. She now is teaching in the School of physics and electronics, Shandong Normal University. Her current research interests are face recognition using Hyper-spectral and deep learning. She has published several high quality papers in international journal.